Numerical Modelling Analysis and Parametric Study of Slim-floor Composite Shear Beams

Xianghe Dai, Dennis Lam, Therese Sheehan, Jie Yang and Kan Zhou

*Faculty of Engineering and Informatics, University of Bradford
Richmond Road, Bradford, UK, BD71DP.
e-mail: x.dai@bradford.ac.uk

Abstract. This paper presents the numerical modelling and analysis of slim-floor composite beam systems using different shear connector arrangements. A finite element model was developed and validated through comparing the prediction with the results obtained from the experimental study. A parametric study was conducted to examine the effect of typical parameters of shear connectors, including the diameter of the concrete dowel cylinder, incorporating dowel reinforcement and concrete strength, etc. The comparison and analysis further clarified the component, mechanism and development of shear resistance and overall load-bearing capacity. The findings based on the numerical simulation provide a deeper insight into the behaviour of this type of slim-floor composite beam system. Through both experimental and numerical studies, the structural merits of this composite beam system were highlighted.

Keywords: Composite beam; slim-floor; concrete dowel; shear connector; numerical modelling.

1 Introduction

Slim-floor composite beams have been increasingly adopted in practice due to their advantages in structural features and construction, such as shallow height and absence of down stand beams. The composite action of the slim-floor beam increases the stiffness of the structural system, however, currently no specific design rules are provided in the Eurocodes to consider this composite action in slim-floor beam systems. The lack of knowledge and understanding might lead to under-estimation of the composite action and the potential of the slim-floor beam system is not fully utilized.

Unlike a conventional composite beam system, in which the composite action is applied via the shear connectors welded at the top flange of the down stand steel beam and embedded in the upper concrete slabs, the composite action of a slim-floor beam system is mainly applied via the dowel shear between the steel and concrete, but the shear resistance may also be acquired via the clamping action between the slab and the steel section as the steel section is directly embedded inside the concrete. For conventional composite beams, the plastic neutral axis is generally designed at or close to the level of the upper concrete slab; therefore the strains in the concrete might be much lower than in the steel section. For slim-floor composite beams, the steel beam section is generally highly asymmetric and therefore the plastic neutral axis might be lower and the strains in concrete slab might be high and cause compression failure. The design rules provided in the current Eurocode 4 for composite construction are not applicable for the structural behaviour of slim-floor beam systems. For example, is the ductility of the shear connectors considered? Should it be based on the minimum slip capacity of 6mm in Eurocode 4? How is the shear resistance of different forms of shear connectors adopted for slim-floor construction? Therefore, further research is needed to understand the performance of slim-floor beam systems, in particular to develop an approach to consider the composite action for the slim-floor design.

In practice, various devices/mechanisms may contribute to the composite action between steel and concrete, such as purpose-built shear connectors, friction and clamping actions. This leads to more complex shear-connection mechanisms than in a conventional composite beam system using welded shear studs. Chen et al. (2015) examined slim-floor beams with innovative transverse shear connectors, and found them to provide an efficient solution, combining the tensile strength of tie bars with the

compressive strength of concrete. Lam et al. (2015) presented a design method for slim-floor construction that comprises a steel beam and a concrete or composite floor slab in which the beam is integrated within the depth of the slab and special attention was paid to the forms of shear connection between steel and concrete. Limazie and Chen (2015) examined the flexural behaviour of composite slim-floor beams considering the effect of parameters such as material strength and geometry. Limazie and Chen (2016, 2017) based on experimental studies, developed FE models and further investigated the flexural behaviour, load-bearing capacity of the composite slim-floor beams and mechanisms of the shear connection through performing parametric studies. Zaharia and Franssen (2012) examined the fire resistance of slim-floor beams utilising horizontal shear studs. Maraveas et al. (2012) and Ellobody (2011) investigated the behaviour of slim-floor beams using profiled metal decking in fire. De Nardin and El Debs (2012) conducted tests on composite connections between slim-floor beams and columns using headed shear studs. Wang et al (2009) studied the load-bearing capacity of composite slim frame beams without specific shear connector devices and design equations were developed.

This paper presents numerical modelling and analysis following a series of slim-floor shear beam tests using various shear connector arrangements carried out in the University of Bradford. FE models were developed using ABAQUS and validated against the experimental observations. A parametric study, covering the dowel hole diameters in the beam web, diameters of rebar shear connectors and concrete strength grades, was conducted. The comparison and analysis highlighted the structural behaviour and performance of slim-floor composite beam systems.

2 Brief Introduction to Experimental Study

In total 8 slim-floor composite beams were tested to investigate their shear behaviour in the University of Bradford. A typical cross-section of a test specimen (SBT5) is presented in Figure 1. Each beam consisted of a HEB200 steel section welded to a 400×15mm steel plate. The HEB-section was embedded in a concrete slab with a total depth of 240 mm (120 mm for upper portion, providing 40 mm cover to the top flange of the steel beam). An A252 steel mesh was placed in the slab above the steel beam to prevent premature cracking of the slab in tension. The shear connector design was based on the concept of dowel action, with 16 mm diameter steel tie bars passing through the 80mm diameter pre-drilled holes with a centre-to-centre spacing of 400mm in the HEB section web, with the concrete dowel between the web hole and bar forming part of the connector. The longitudinal shear force was transmitted between the steel and concrete elements. In addition to the dowel shear reinforcement, the friction/adhesion and clamping between the steel and concrete also contributed to the shear transfer. Once the applied load exceeded the shear resistance of the concrete core, a large slip occurred between the slab and the steel section, which then activated the dowel action in the transverse shear connectors. Transmission of the longitudinal shear force through these bars was vital in ensuring a ductile performance of the slim-floor system.

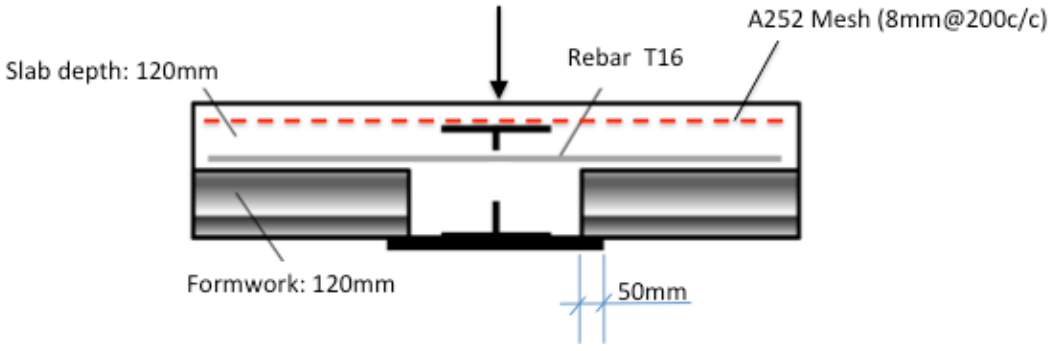

Figure 1. A typical composite slim-floor beam section (SBT5)

All specimens were 4300 mm long (4000 mm between the supports). Loading was applied at two points along the longitudinal direction, at 1.5 m from each end, as shown in Figure 2. At these locations, loading was either applied at one point in the centre of the cross-section (concentric loading), or at two points, one at each side of the section, at a 300 mm eccentricity from the centre (eccentric loading). Grade S355 steel was used for the HEB section and bottom steel plate, with a yield strength and ultimate strength of 428MPa and 519MPa respectively for the HEB200 section and 455MPa and 525MPa respectively for the bottom plate. C25/30 concrete was used for the slab and the average measured compressive cube strength was 42.5N/mm^2 for SBT1(a,b), SBT2, SBT3, SBT5 and SBT7 and 34.1 N/mm^2 for SBT4 and SBT6 N/mm^2. Details of the test specimens and test programme may be found from the publication Sheehan, et al (2019).

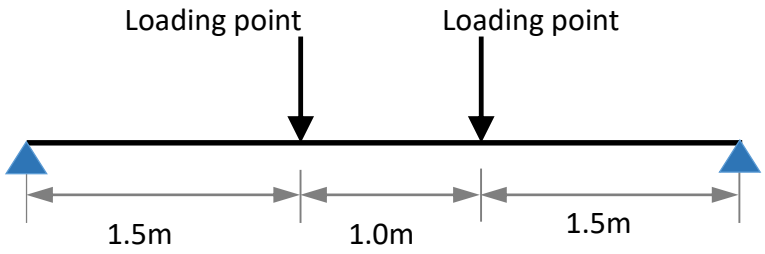

Figure 2. Location of loading points along beam length

The experimental study indicated that all of the slim-floor beams exhibited a ductile response, undergoing a mid-span deflection exceeding span/50 despite some of the beams being designed with a low degree of shear connection. The response of specimens under eccentric loading was similar to that of specimens under concentric loading. The overall performance of specimens using transverse bars was similar to that of specimens using lying shear studs l although some differences were noted in the strain distribution. A degree of shear connection in the region of 17 % could be achieved without the use of specific shear connectors, by relying on clamping action and friction alone. The concrete dowel provided a significant contribution to the longitudinal shear resistance, with specimens using larger web openings resisting a greater overall maximum load. The concrete cover above the steel top flange played an important role in providing shear connection through clamping and friction effects. The increased concrete dowel increased the shear connector capacity, but appeared to significantly reduce the shear connection provided by clamping action/friction. The test programme did not investigate the effect of concrete strength on the load-bearing capacity and structural behaviour of the slim-floor composite beams. The test programme only considered the 40mm and 80mm dowel hole and the shear rebar diameter of 16mm. Therefore, the study presented in the following sections would complement the previous experimental study. A numerical model was developed and validated, and a parametric study was conducted investigating the effects of dowel hole diameter, rebar diameter and concrete strength on the structural behaviour of this type slim-floor beam system.

3 FE Model Development and Validation

3.1 Description of the FE modelling

Although full-scale specimen testing may provide reliable results for structural behaviour of slim-floor beam systems, it is costly and time consuming. To further understand the slim-floor system and extend the database, FE models, through an ABAQUS general standard analysis approach, were developed and validated against the experimental observations before a parametric study was conducted. Considering the symmetrical conditions of the structure across the centrelines of the overall slim-floor beam and the symmetrical loading arrangement, only a quarter of the geometry of the tested specimen was modelled to save computational time. The main components of the FE model included the concrete slab, steel beam section, reinforcement steel mesh, rebar shear connectors incorporating the dowel hole on the

steel beam web, shear studs welded at the steel beam web (only specimens SBT6), and additional reinforcement stirrups (only specimen SBT1a). The components were created separately and then assembled, as shown in *Figure 3* and *Figure 4*, to form the slim-floor beam structure tested in the University of Bradford.

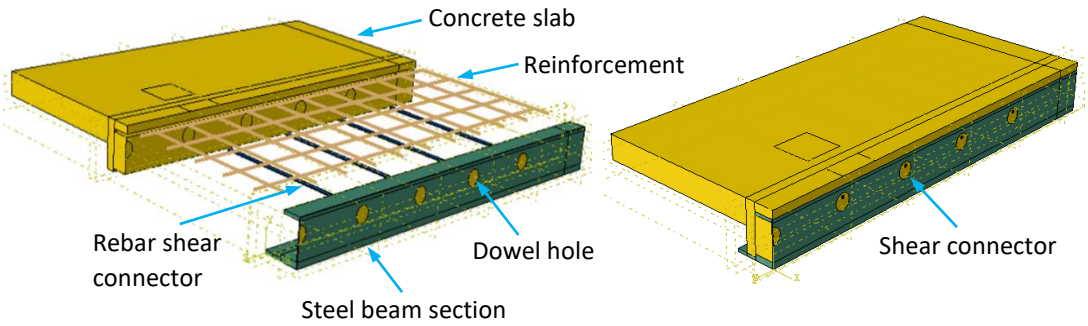

Figure 3: Component creation and assembly of a quartered tested specimen

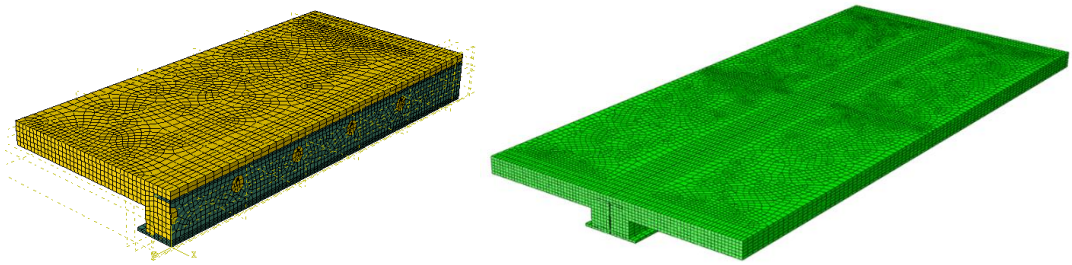

Figure 4: View of the finite element mesh

3.2 Element type and mesh

Three dimensional eight-node solid brick elements with reduced integration (C3D8R) were adopted to mesh the concrete slab, steel beam, shear connector rebar and shear studs. For this type of element, each node has three translational degrees of freedom (DOF) and shear locking can be prevented through reduced integration. In addition, the brick elements might give a solution of comparable accuracy at a better rate of convergence and less computational time needed than using some other types of elements. The two-node truss element (T3D2) was used for the reinforcement steel mesh and reinforcement steel stirrups in specimen SBT1b. The truss element in ABAQUS can be used in two or three dimensions to present a slender structural element that resists and transfers only axial force. The advantage of using truss elements is that the perfect-bond can easily be defined by embedding the steel bars into the concrete slab (the host region). For the main components, the steel beam and concrete slab, a sensitivity study showed that element sizes of 50mm in the axial direction and 25mm in the transverse direction gave the best agreement compared with the experimental observations.

3.3 Interaction contact and constraint

Once all parts of the shear beam system were assembled in FE model as shown in *Figure 3*, the appropriate contact interactions were defined between interacting surfaces of different components. For contact between the concrete slab and the steel beam section, the normal behaviour was assumed to be "hard" as this type of contact behaviour allows only very little penetration of the slave surface into the master surface. The "penalty" method was used to define the tangential slip where a friction coefficient of 0.2 was adopted, which provided a satisfactory degree of accuracy when compared with the experimental results after a sensitivity study was performed on friction coefficients ranging from 0.1 to

0.5. The reinforcement steel mesh, rebar shear connector and shear stud were "embedded" into the concrete slab to simplify the modelling.

3.4 Material Properties

The steel beam section including the welded bottom plate was of grade S355 with Young's modulus assumed to be 210 GPa and Poisson's ratio assumed to be 0.3. For the reinforcement steel mesh/rebar connector/stirrup, both the yield strength and the ultimate strength were assumed to be 500 N/mm^2, with a Young's modulus of 210 GPa and a Poisson's ratio of 0.3. For the shear studs, a yield strength of 420 N/mm^2 and an ultimate strength of 610 N/mm^2 were used based on a test carried in the University of Bradford.

For the concrete, the target grade for the tested specimens should be C25/30, however the test day measurements showed that for most specimens the average compressive cube strength was higher (41.3-43.9 N/mm^2) although for SBT4 and SBT6 the measured compressive strength was 34.1 N/mm^2. Therefore in the FE modelling, an average compressive strength of 42.5N/mm^2 was adopted for SBT1(a,b), SBT2, SBT3, SBT5 and SBT7; the strength of 34.1 N/mm^2 was adopted for SBT4 and SBT6. A concrete damage plasticity (CPD) constitutive model was employed and the concrete maximum tensile strength was assumed to be 10% of the maximum compressive strength.

3.5 FE model validation and comparison/analysis

Figure 5 compares the predicted mid-span deflection vs. load relationships and end slip vs. load relationships with the experimental results for three typical specimens SBT2, SBT5 and SBT7. It can be seen that the comparisons between FE predictions and experimental results show good agreements. Although in some cases, the modelling did not fully catch the structural performance, such as in SBT2, the prediction did not exactly reflect the sudden drop of stiffness and the end slip behaviour before the load reached about 500 kN, whereas, the experimental observations showed clear changes in load-bearing capacity and stiffness at end slips of 10-20 mm. This was possibly because the formation of the cracks in concrete caused the static friction between steel and concrete to be overcome and the bond condition to be changed. However, the FE prediction clearly captured the general load-deflection and load-end slip behaviour. Additionally, the end slips measured at both ends in some tests were different due to geometric imperfections of the tested specimens and possible asymmetry of the loading, but the FE modelling could not simulate this feature as observed from the tests. As clarified, the differences between the numerical predictions and experimental observations might have resulted from the tolerance of the tested specimens which included the specimen member imperfection and test setup tolerance, etc., but the FE model employed the ideal boundary conditions and loading procedure, perfect set up, uniform material distribution and ideal bond conditions, etc.. *Table 1* further compares the load-bearing capacities predicted by the FE modelling and measured from experiments at 30mm, 60mm mid-span deflections and 6mm end-slip, it is found that they are very close with the average test-to-modelling ratio being 0.96 at 30mm mid-span deflection and 0.99 at both 60 mm mid-span deflection and 6 mm end-slip. *Figure 6* compares the visible deformation of the slim-floor composite beam system including the mid-span vertical deflection, crack distribution/development and end-slip between the steel beam section and wrapped concrete. Obviously, the FE modelling successfully captured these key features. Through the above comparison, it may be concluded that the FE model can be used to simulate similar composite beam systems and carry out a parametric study.

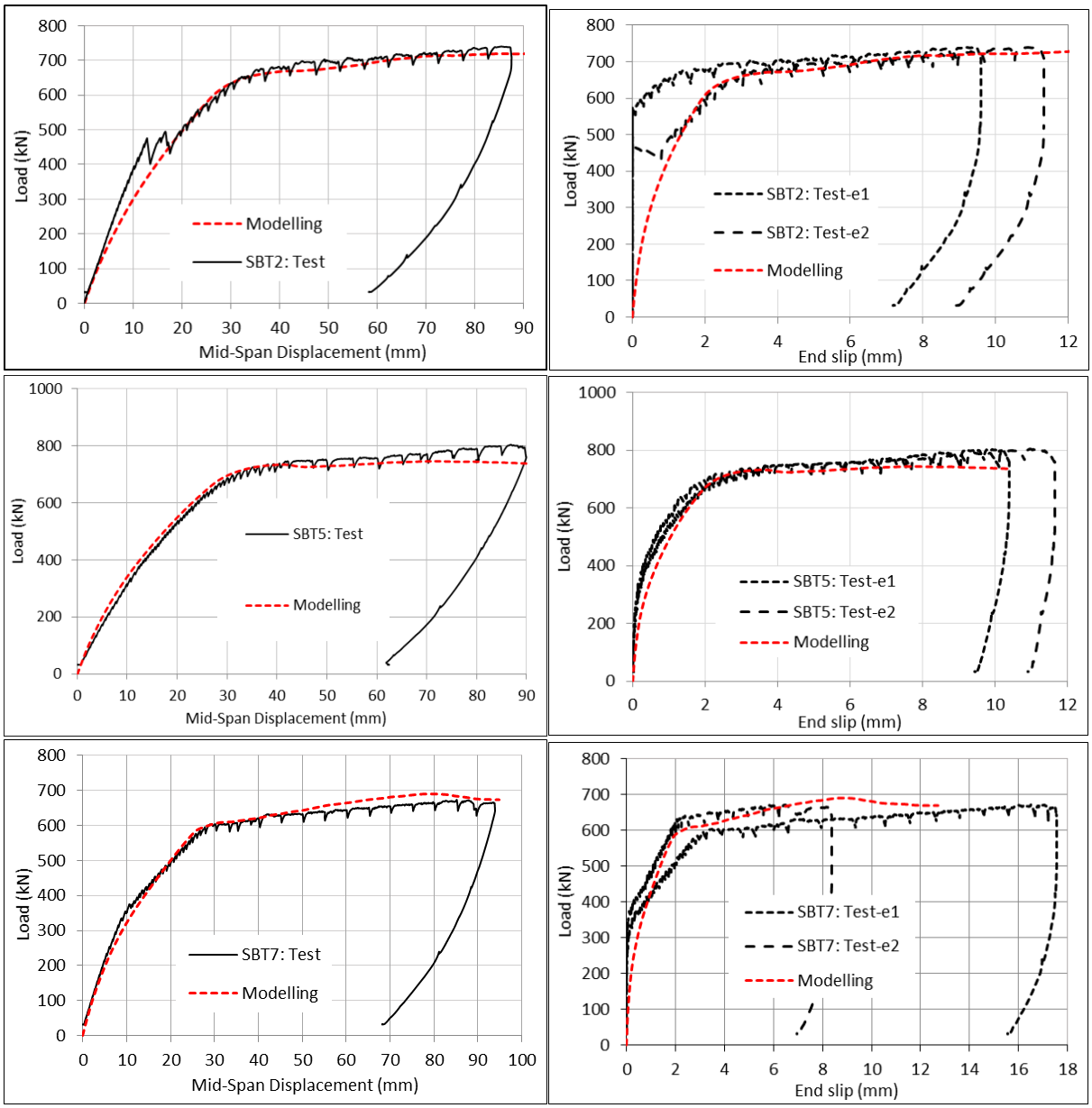

Figure 5: Comparison of mid-span deflection obtained from FE prediction and test observation

Table 1: Comparison of load-bearing capacity at 30 and 60mm mid-span deflection and 6mm end slip

Specimen ID	Load (kN) at 30 mm mid-span deflection			Load (kN) at 60 mm mid-span deflection			Load (kN) at 6 mm end slip		
	P_{test}	P_{FE}	P_{test}/P_{FE}	P_{test}	P_{FE}	P_{test}/P_{FE}	P_{test}	P_{FE}	P_{test}/P_{FE}
SBT1a	615	672	0.915	712	709	1.004	695	700	0.993
SBT1b	600	630	0.952	685	701	0.977	680	684	0.994
SBT2	635	636	0.998	703	697	1.009	700	690	1.014
SBT3	510	497	1.026	536	535	1.002	522	520	1.004
SBT4	500	550	0.909	575	580	0.991	585	604	0.969
SBT5	686	695	0.987	740	737	1.004	756	736	1.027
SBT6	635	685	0.927	708	701	1.010	700	703	0.996

SBT7	603	605	0.997	641	664	0.965	630	661	0.953
Average			0.964			0.995			0.994

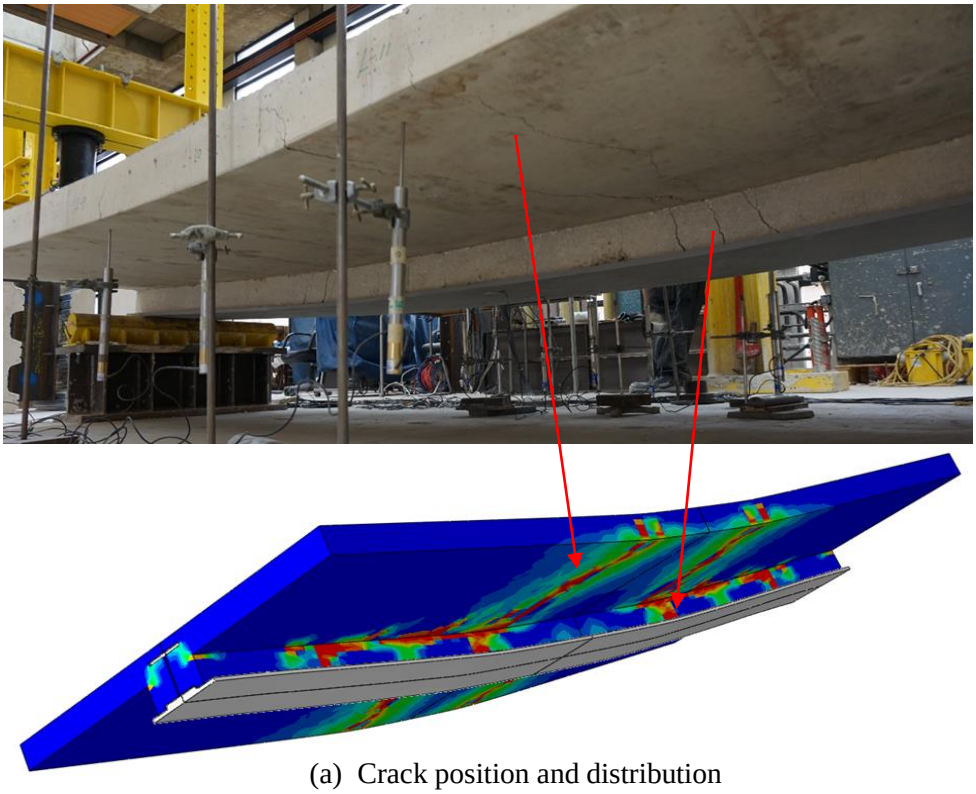

(a) Crack position and distribution

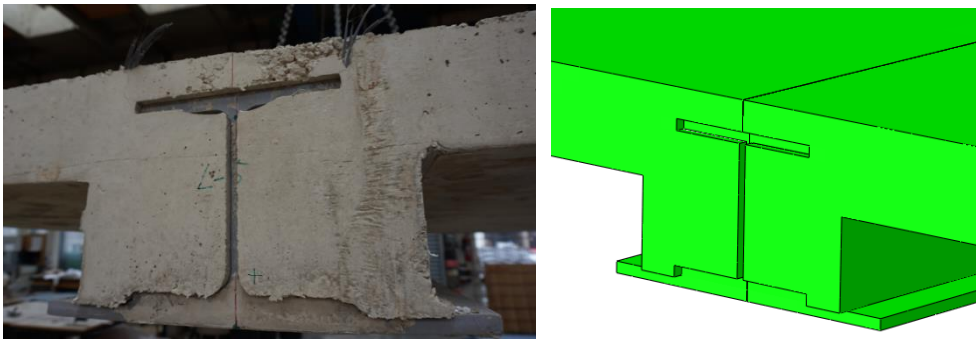

(b) End slip between steel beam and concrete

Figure 6: Comparisons of concrete slab crack/damage development between test observations and FE predictions

4 Parametric study

4.1 Effect of concrete dowel diameter on load-bearing capacity

The difference between SBT1a, SBT1b, SBT2 and SBT5 was the dowel hole diameter in the steel beam web. The experimental results demonstrated that a higher capacity was achieved when a bigger dowel hole diameter was adopted (SBT5). Therefore, to investigate the effect of the concrete dowel shear resistance on the load-bearing capacity of the slim-floor beam system, a parametric study was carried out using the above described FE modelling method considering the following dowel hole diameters: 0 mm (no dowel hole used and therefore no rebar shear connector in this case), 40mm, 80mm, 100mm, 120mm and 160mm. The FE model was established based on the SBT5 test specimen, whose concrete compressive cube strength was 42.5 N/mm^2, the cooperating rebar shear connector diameter was 16mm and the composite beam was centrally loaded. *Figure 7* compares the load versus mid-span deflection curves and load versus end slip behaviours of the slim-floor beam systems with different dowel hole diameters. It was obvious that different dowel hole diameters resulted in different beam performances, and the composite beam without dowel holes, i.e., without rebar shear connectors, had the lowest load-bearing capacity. The beam systems with dowel hole diameters ranging from 80 to 120 mm had the highest load-bearing capacities followed by the beam systems with dowel hole diameters of 40 or 160mm.

The experimental results of specimens SBT5 and SBT7 (of same diameter of dowel hole) clearly indicated that without the use of rebar shear connectors SBT7 had a lower load-bearing capacity. Therefore, the effect of the dowel hole diameter of slim-floor beams without incorporating rebar shear connectors was also considered in the parametric study. The FE model was identical to the FE model for the beam system with rebar shear connectors, except that the rebar shear connectors were removed in this parametric study. The comparison is shown in *Figure 8*. Similar to slim-floor beams with rebar shear connectors, composite beam without a dowel holes (D=0), thus without concrete dowel shear connectors, had the lowest load-bearing capacity. Beam systems with dowel hole diameters of 80-120 mm had the highest load-bearing capacities followed by the beam systems with dowel hole diameters of 40 or 160 mm.

As aforementioned in the summary of the experimental study, the longitudinal shear resistance from the concrete dowel cylinder, rebar shear connector, the friction/adhesion and clamping between the steel and concrete may contribute to the overall load-bearing capacity of the slim-floor beam system. It is clear that a bigger dowel hole might provide a higher shear resistance; however, the bigger dowel hole in the steel beam web might directly impair the load-bearing capacity of the steel section. To explore the effect of dowel hole size on the load-bearing capacity of individual beams, another set of FE models considering dowel holes of different diameters, was developed. *Figure 9* compares the load-bearing capacity of steel beams with different dowel hole diameters. It can be seen as the dowel hole diameter increased, the steel beam load-bearing capacity decreased. This might partially explain the reason that for slim-floor beams with 160 mm dowel holes, the overall load-bearing capacity was lower than that of slim-floor beams with 120 mm dowel holes although the concrete dowel shear resistance increased.

Figure 10 and *Table 2* further compare the load-bearing capacities of slim-floor beams with different dowel hole diameters at 30 mm and 60 mm mid-span deflections. It can be seen, regardless of the use of rebar shear connectors, the beam systems with dowel holes of 80-120 mm have higher resistance and therefore is recommended to be used in practice. It appears the 100 mm dowel hole shows the best performance. It has been noticed that beam systems using solid steel sections have the lowest load-bearing capacity due to the lack of dowel shear resistance. Certainly, besides the concrete dowel action, the rebar shear connector provided effective shear resistance, therefore the load-bearing capacity of beam systems with rebar is higher than those without rebar shear connectors. Clearly, for the beam systems with the largest dowel holes of 160 mm, the resistance from shear connectors increased while

the bearing load from the steel section itself was reduced. Therefore, the optimum slim-floor beam system needs to consider the effects of both steel section and dowel resistance.

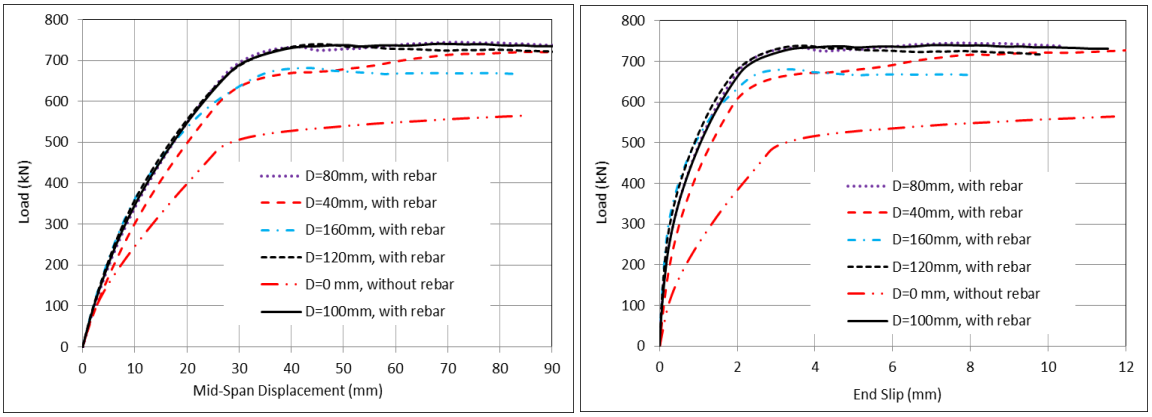

Figure 7: Load-bearing capacity of slim-floor beam with different dowel hole diameters (with shear connector rebar T16)

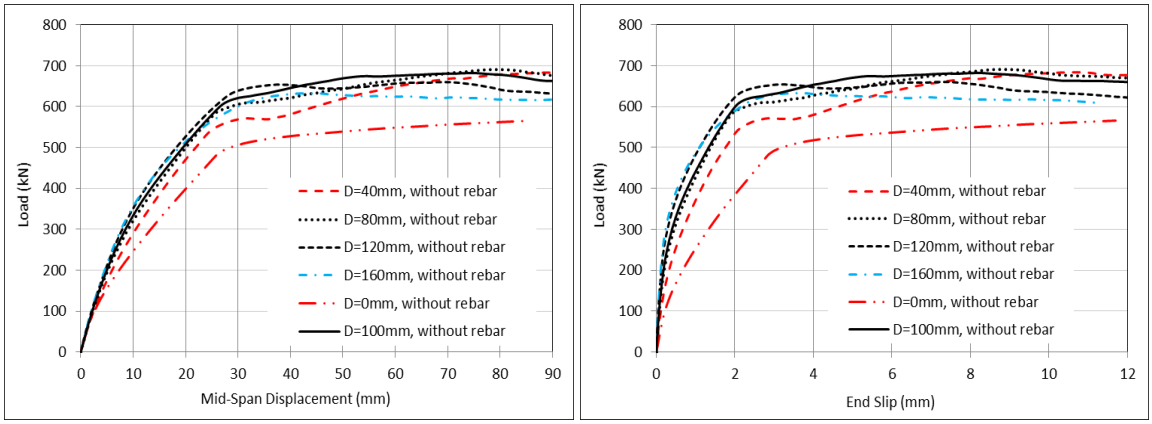

Figure 8: Load-bearing capacity of slim-floor beam with different dowel hole diameters (without shear connector rebar)

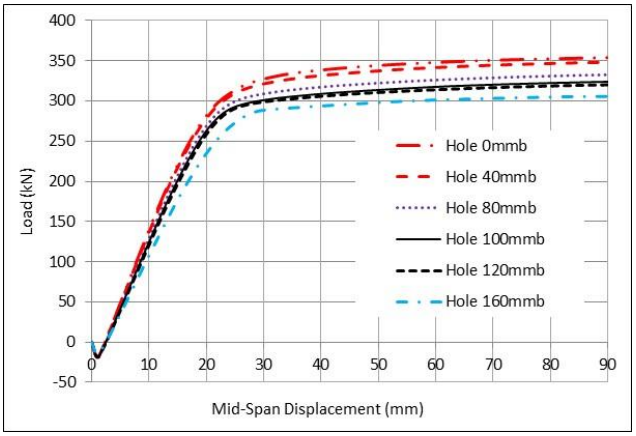

Figure 9: Effect of dowel hole diameter on the load-bearing capacity of the steel beam section

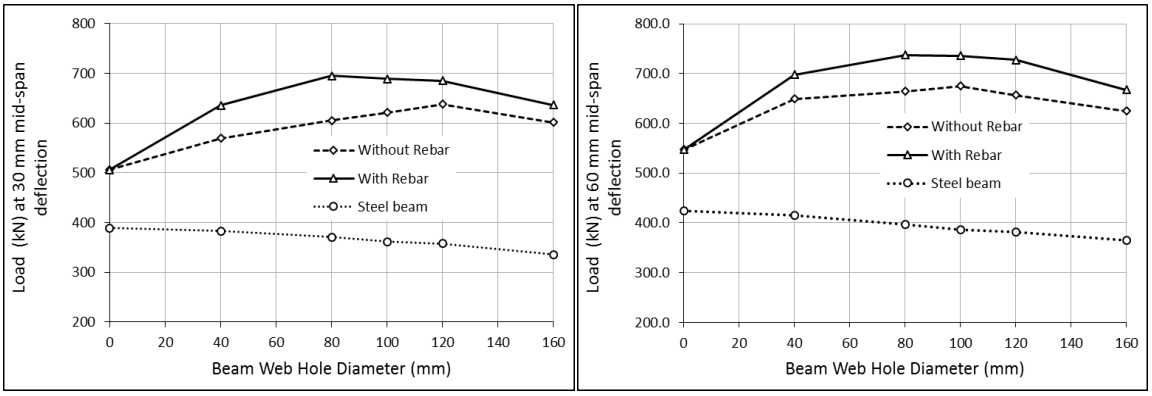

Figure 10: Comparison of load-bearing capacity of slim-floor beams with different dowel hole diameters at 30/60 mm mid-span deflection

Table 2: Summary of load-bearing capacities of slim-floor beams with various dowel hole diameters at 6mm end slip, 30 and 60mm mid-span deflections

Specimen ID/feature	Dowel hole diameter (mm)	Load-bearing capacity at 6mm end slip			Load-bearing capacity at 30mm mid-span deflection			Load-bearing capacity at 60mm mid-span deflection		
		P (kN)	P/P_0	Mid-span deflection (mm)	P (kN)	P/P_0	End slip (mm)	P (kN)	P/P_0	End slip (mm)
Specimens **without** rebar shear connector of 16mm diameter passing the the hole	0	493.5	1.00	47.7	488.6	1.00	3.22	502.0	1.00	8.1
	40	637.3	1.29	55.6	569.5	1.17	2.66	649.3	1.29	6.56
	80	660.7	1.34	57.9	604.8	1.24	2.44	664.1	1.32	6.27
	100	674.5	1.37	58.3	621.2	1.27	2.4	674.6	1.34	6.2
	120	656.1	1.33	59.7	637.5	1.30	2.22	656.4	1.31	6.03
	160	623.7	1.26	64.7	601	1.23	2.18	624.8	1.24	5.43
Specimens **with** rebar shear connector of 16mm diameter passing the the hole	0	493.5	1.00	47.7	488.6	1.00	3.22	502.0	1.00	8.1
	40	697	1.41	57.3	635.2	1.30	2.34	697.6	1.39	6.37
	80	735.8	1.49	58.6	694.5	1.42	2.22	737.1	1.47	6.18
	100	736.6	1.49	59.9	688.5	1.41	2.2	736	1.47	6.02
	120	726.5	1.47	64.2	685	1.40	2.04	727.6	1.45	5.43
	160	668	1.35	65.9	636	1.30	2.02	667	1.33	5.33
Only Steel beam section	0				327.6	1.00		348.4	1.00	
	40				321.4	0.98		341.5	0.98	
	80				309.1	0.94		326.3	0.94	
	100				301.2	0.92		317.6	0.91	
	120				298.6	0.91		313.6	0.90	
	160				288.6	0.88		301.2	0.86	

4.2 Effect of diameter of rebar shear connector on load-bearing capacity

To further investigate the influence of the incorporated rebar shear connector on the beam behaviour, a parametric study was conducted. The FE model was based on the SBT5 specimen and four rebar diameters: 12 mm, 16 mm, 20 mm and 24 mm, were considered. *Figure 11* shows the load vs. mid span deflection relationships and load vs. end slip relationships. It can be seen that as the rebar diameter

increased, the load-bearing capacity increased. *Figure 12* and *Table 3* further compare the load-bearing capacity at 30/60 mm mid span deflections and at 6 mm end slip. It can be found that at 30 mm mid-span deflection, the load-bearing capacity increased by about 2% as rebar diameter increased by 4 mm. At 60 mm mid-span deflection or 6 mm end slip, the load-bearing capacity increased by about 3% when the bar diameter increased by 4 mm.

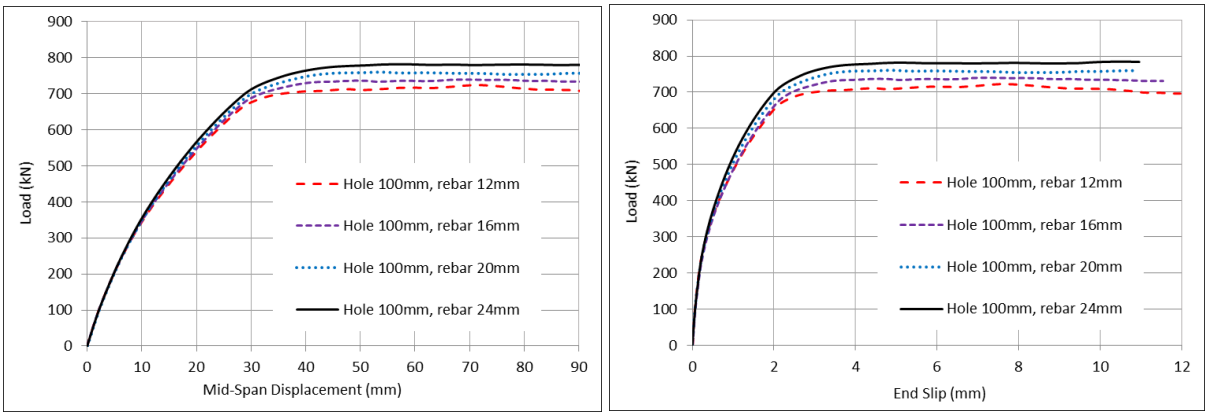

Figure 11: Load vs mid span deflection and end slip of beam systems with different rebar diameters (with dowel hole diameter of 100mm)

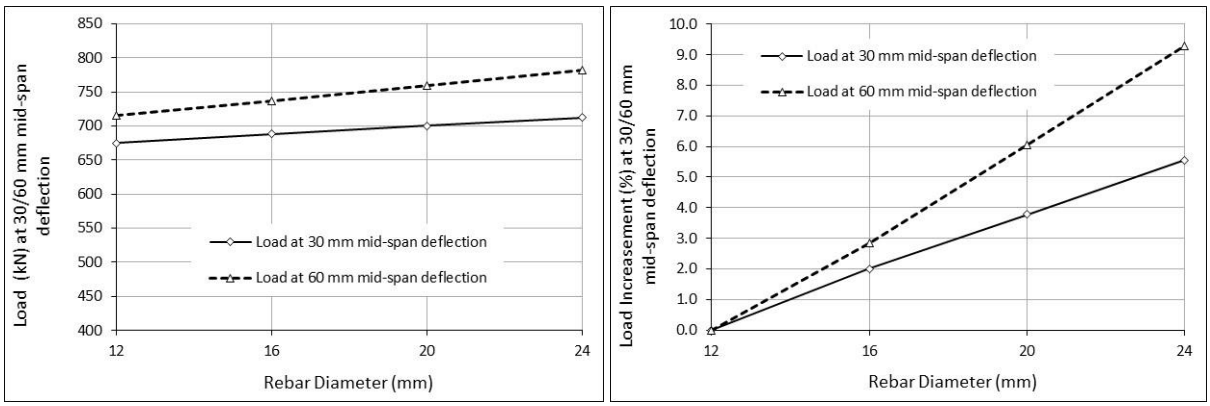

Figure 12: Effect of rebar diameter on the load-bearing capacity (with dowel hole diameter of 100mm)

Table 3: Summary of load-bearing capacities of slim-floor beams with different rebar diameter at 6mm end slip, 30 and 60mm mid-span deflection

Specimen ID	Rebar shear connector diameter (mm)	Load-bearing capacity at 6mm end slip			Load-bearing capacity at 30mm mid-span deflection			Load-bearing capacity at 60mm mid-span deflection		
		P (kN)	P/P_{12}	Mid-span deflection (mm)	P (kN)	P/P_{12}	End slip (mm)	P (kN)	P/P_{12}	End slip (mm)
Composite beam with dowel hole of 100 mm	12	716	1.00	59.40	675	1.00	2.23	716	1.00	6.06
	16	736	1.03	60.00	688.5	1.02	2.22	736	1.03	6.02
	20	759	1.06	62.00	700.5	1.04	2.17	759	1.06	5.73
	24	780	1.09	64.00	712.5	1.06	2.13	782	1.09	5.41

4.3 Effect of concrete strength on load-bearing capacity

Since the concrete dowel cylinder made a significant contribution to the shear resistance of the slim-floor beam system, a parametric study was performed to investigate the effect of concrete by varying only the concrete strength. FE models were established based on different testing specimens as listed in *Table 1*. Four different concrete grades were employed in the parametric study, with the compressive cylinder strengths being 20 N/mm^2, 30 N/mm^2, 40 N/mm^2 and 50 N/mm^2.

Figure 13 presents typical load vs. mid-span deflection and load vs. end-slip curves of the composite beam system (SBT7) with different concrete strengths adopted. As expected, the higher the concrete strength, the higher the beam stiffness and the beam load-bearing capacity. *Figure 14* and *Table 4* compare the load-bearing capacity of different specimens with various concrete strengths at 30/60 mm mid-span deflection and 6 mm end slip. It can be seen, as observed from the experimental study, regardless of concrete strength, SBT1b, SBT2 and SBT5 had higher load-bearing capacities, followed by SBT6, SBT7, SBT4. The SBT3 series had the lowest load-bearing capacity. The comparison clearly shows the important influence of the rebar shear connector, concrete dowel (cylinder) shear resistance and dowel diameter on the behaviour of the slim-floor composite beam system.

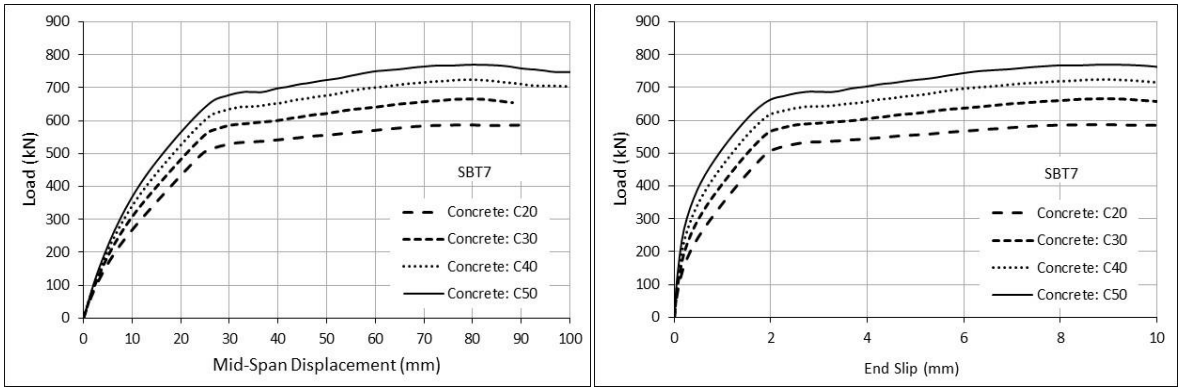

Figure 13: Load vs. mid span deflection/end slip of SBT7 with varying concrete strength

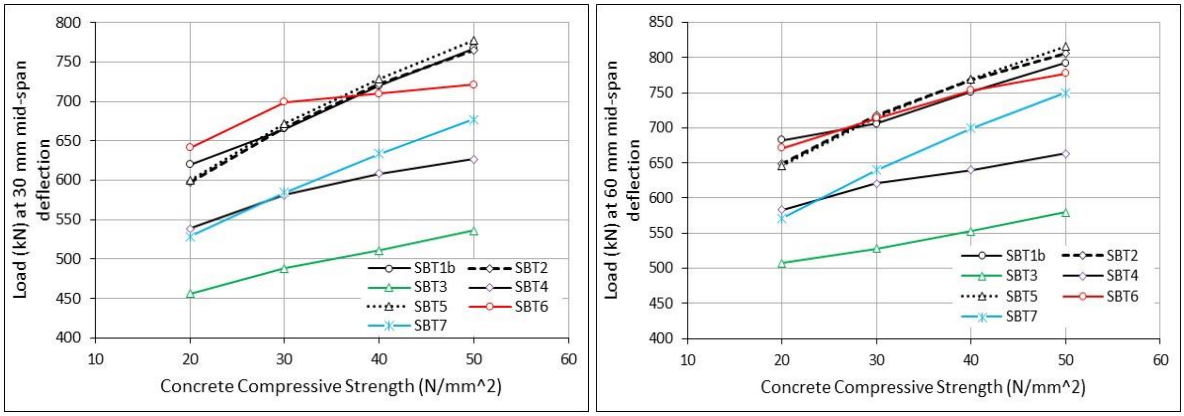

Figure 14: Effect of concrete strength on the load-bearing capacity of different specimens at 30mm and 60mm mid-span deflection

Table 4: Summary of load-bearing capacities of slim-floor beams with various concrete strengths at 6mm end slip, 30 and 60mm mid-span deflection

Specimen ID	Concrete cylinder strength (N/mm2)	Load-bearing capacity at 6mm end slip			Load-bearing capacity at 30mm mid-span deflection			Load-bearing capacity at 60mm mid-span deflection		
		P (kN)	P/P_{20}	Mid-span deflection (mm)	P (kN)	P/P_{20}	End slip (mm)	P (kN)	P/P_{20}	End slip (mm)
SBT1b	20	683.7	1.00	61.3	619.6	1.00	2.2	682.5	1.00	5.84
	30	712.7	1.04	67.6	665	1.07	1.64	705.6	1.03	5.12
	40	758	1.11	67.1	720	1.16	1.64	751	1.10	5.21
	50	802.1	1.17	68.3	767.2	1.24	1.59	792	1.16	5.14
SBT2	20	656.2	1.00	68.7	598	1.00	1.75	649.3	1.00	5.02
	30	724	1.10	68.1	666.5	1.11	1.71	718	1.11	5.05
	40	776.3	1.18	68.8	722.5	1.21	1.66	767.5	1.18	5.05
	50	822	1.25	69.4	765	1.28	1.62	805.5	1.24	5.02
SBT3	20	502.7	1.00	56.4	456	1.00	2.67	507.6	1.00	6.44
	30	523.2	1.04	55.4	488.2	1.07	2.67	527.9	1.04	6.6
	40	547.6	1.09	55.2	511	1.12	2.66	552.7	1.09	6.65
	50	575.8	1.15	56	535.8	1.18	2.61	579.5	1.14	6.47
SBT4	20	593.5	1.00	79.8	538.8	1.00	1.38	583	1.00	4.19
	30	632.1	1.07	79.5	581.2	1.08	1.39	620.7	1.06	4.22
	40	657.2	1.11	79.5	608.4	1.13	1.4	640	1.10	4.17
	50	679.4	1.14	79.2	627	1.16	1.4	663	1.14	4.26
SBT5	20	653.7	1.00	67.6	600.5	1.00	1.73	646.4	1.00	5.1
	30	720.7	1.10	67.3	671.5	1.12	1.68	715.2	1.11	5.11
	40	769.6	1.18	59.8	729	1.21	2.12	769.8	1.19	5.95
	50	816.7	1.25	61.6	777.2	1.29	2.03	816	1.26	5.68
SBT6	20	671	1.00	60.3	641	1.00	1.9	670.9	1.00	6.03
	30	717.1	1.07	63.7	699.3	1.09	1.51	713.4	1.06	5.48
	40	754.9	1.13	62	710	1.11	1.82	753	1.12	5.73
	50	777	1.16	60.1	721.3	1.13	1.96	777	1.16	5.96
SBT7	20	576.8	1.00	57.6	528.5	1.00	2.51	571	1.00	6.31
	30	637	1.10	57.6	584.5	1.11	2.48	640	1.12	6.3
	40	695.1	1.21	57.5	633.5	1.20	2.42	699.5	1.23	6.32
	50	744.1	1.29	57.7	677	1.28	2.36	749.6	1.31	6.16

5 Conclusions

Following the slim-floor shear beam tests carried out in the University of Bradford, FE models, using ABAQUS software with a concrete damaged plasticity (CDP) material constitutive model, were developed. The FE modelling method was successfully validated against the experimental observations. A comprehensive parametric study, covering the dowel hole diameter, diameter of rebar shear connector and concrete strength, was conducted. The parametric study deepened the understanding of the effects of various parameters on the behaviour of slim-floor composite beam systems. Based on the numerical simulation, comparison and analysis, the following conclusions can be drawn;

(1) The FE model developed through ABAQUS software could be used to capture the main structural behaviour and failure modes of the slim-floor composite beam including load-bearing capacity, deflection, slip behaviour and concrete cracking distribution, etc.
(2) The dowel hole in the steel beam web played an important role in the load-bearing capacity of the slim-floor beam system. The larger the hole, the higher the shear resistance that was provided by the concrete cylinder. However, since the larger hole caused more area reduction to the web of the steel section, it reduced the load-bearing capacity of the steel section, and therefore for the described slim-floor composite beam system, the optimum hole diameter is recommended to be from 80 mm to 120 mm based on the limited cases considered in this study. The 100mm dowel hole might allow the beam system to have the best load-bearing capacity and structural performance regardless of whether rebar shear connectors are adopted or not.
(3) Furthermore, the diameter of the incorporating rebar shear connector affected the load-bearing capacity. For the described slim-floor beam system, considering a rebar diameter ranging from 12 mm to 24 mm, the load-bearing capacity was found to increase by 2-3% if the rebar diameter increased by 4 mm.
(4) As expected, the concrete strength had a significant effect on the load-bearing capacity and slip behaviour. The higher the concrete strength, the higher the load-bearing capacity that the composite beam system might reach.

6 Acknowledgement

The research leading to these results is part of a joint project of the University of Bradford, the University of Stuttgart, the University of Trento, the Steel Construction Institute, ArcelorMittal and Lindab S.A. The authors gratefully acknowledge the funding received from the European Community Research Fund for Coal and Steel under grant agreement number RFSR-CT-2015-00020.

References

Chen S, Limazie T and Tan J. (2015). Flexural behavior of shallow cellular composite floor beams with innovative shear connections. Journal of Constructional Steel Research, 106: 329-346.
De Nardin, S. and El Debs, A. L. H. C. (2012), Composite connections in slim-floor system: An experimental study, Journal of Constructional Steel Research 68(1): 78-88
EN 1994-1-1: Eurocode 4 - Design of composite steel and concrete structures. Part 1-1: General rules and rules for buildings. Brussels, Belgium: European Committee for Standardization (CEN); 2004.
Ellobody, E. (2011), Nonlinear behaviour of unprotected composite slim floor steel beams exposed to different fire conditions, Thin-Walled Structures 49(6): 762-771.
Lam, D., Dai, X., Kuhlmann, U., Raichle, J. and Braun, M. (2015) Slim-floor construction – design for ultimate limite state, Steel Construction 8(2): 79-84
Limazie, T. and Chen, S. (2015), Numerical procedure for nonlinear behavior analysis of composite slim floor beams, Journal of Constructional Steel Research 106: 209-219.
Limazie, T. Chen, S. (2016), FE modeling and numerical investigation of shallow cellular composite floor beams, Journal of Constructional Steel Research 119: 190–201.
Limazie, T. Chen, S. (2017), Effective shear connection for shallow cellular composite floor beams, Journal of Constructional Steel Research 128: 772–788.
Maraveas, C., Swailes, T. and Wang, Y. (2012). A detailed methodology for the finite element analysis of asymmetric slim floor beams in fire, Steel Construction 5(3): 191-198.
Sheehan, T., Dai, X., Yang, J., Zhou, K. and Lam, D. (2019). Shear Behaviour of Slim Floor composite beams. Structures, in press.
Wang, Y. Yang, L. Shi, Y. Zhang, R. (2009), Loading capacity of composite slim frame beams, Journal of Constructional Steel Research 65: 650-661
Zaharia, R. and Franssen, J. M. (2012). Simple equations for the calculation of the temperature within the cross-section of slim floor beams under ISO fire, Steel and Composite Structures 13(2): 171-185.